The Astrophysical Journal, 657:486–493, 2007 March 1

CHROMOSPHERIC ACTIVITY IN G AND K MAIN-SEQUENCE STARS, AND WHAT IT TELLS US ABOUT STELLAR DYNAMOS

Erika Böhm-Vitense
Astronomy Department, University of Washington, Seattle, WA
Received 2006 September 7; accepted 2006 October 29

ABSTRACT

For main-sequence G and K stars we study again the empirical relations between the periods of the activity cycles, P_{cyc}, and the rotational periods, p_{rot}. We use the high-quality data selected by Brandenburg, Saar, and Turpin. As found by those authors "the P_{cyc} increase proportional to the p_{rot}, along two distinctly different sequences," the active "A" sequence, and the inactive "'I" sequence with cooler and more slowly rotating stars. It is found here that along each sequence the number of rotation periods per activity cycle is nearly the same, but the numbers are different for the different sequences, indicating that probably different kinds of dynamos are working for the stars on the different sequences. The transition from one sequence to the other occurs at a rotation period of 21 days. The rotation periods then increase abruptly by about a factor of 2 for the cooler stars. We suggest that this indicates abruptly increased deep mixing. Along the I sequence the overall dependence of the Ca II emission line fluxes, F(Ca II), on rotation and T_{eff} is consistent with $F(\text{Ca II}) \propto T_{eff}^4 p_{rot}^{-4/3}$. For the A-sequence stars the dependence of F(Ca II) on rotation seems to be stronger than for the I-sequence stars.

Subject headings: stars: activity — stars: chromospheres — stars: late-type — stars: rotation

1. INTRODUCTION

The relation between the lengths of the activity cycles for stellar chromospheres and coronae and stellar parameters such as T_{eff} and rotation periods has been studied and discussed for several decades. It is well known that solar activity is caused by magnetic fields (Babcock 1958). Following an original suggestion by Babcock (1961), it is usually assumed that the intensification of magnetic fields by a stellar dynamo is due to latitudinal velocity gradients, seen on the surface of the Sun as the differential rotation. This is created by the interaction of rotation and convection. As emphasized by Brandenburg (1998), vertical velocity gradients, due to different rotational velocities in different depths, can also lead to dynamos. Weber & Davis (1967) showed that stellar winds in the presence of magnetic fields can brake rotation on the stellar surface. This leads to outward decreasing rotational velocities, creating vertical velocity gradients. Large-scale motions in the stars, leading to redistribution of angular momentum (see Endal & Sofia 1968; Böhm-Vitense 2004), also lead to vertical gradients of rotational velocities, which are largest at the bottom of the mixed layers. From helioseismology Benevolenskaya et al. (1999) derived that in the Sun the largest gradients in rotation rates are found near the surface and at the bottom of the convective layer, especially at low latitudes (see Brandenburg 2005, Fig. 1). There are thus two regions in solar-type stars where stellar dynamos may work: near the surface, where differential rotation is seen, and where according to Benevolenskaya et al. (1999) the rotation velocity decreases outward, and at the bottom of the convective or otherwise mixed layer.

In stars, magnetic fields are frozen in the material. In the presence of rotational velocity gradients rotation therefore winds up magnetic field lines and creates an increasing toroidal magnetic field until the magnetic buoyancy is strong enough to overcome the resisting forces and brings the toroidal field to the surface. This leads to the surface activity. We suggest here that the time it takes to reach the rising point for the toroidal field determines the length of the activity cycles. Therefore the relation between the lengths of the rotation periods, p_{rot}, and the cycle lengths, P_{cyc}, may tell us which velocity gradients are the most important ones for the stellar dynamo(s) that lead to the solar and stellar activities.

Wilson (1978), Baliunas & Vaughan (1985), Baliunas et al. (1995), and others have devoted major parts of their research efforts to the determination of p_{rot} and P_{cyc}, studying the temporal variations of the Ca II emission lines and photometric variations. Brandenburg et al. (1998) critically discussed the available data. Saar & Brandenburg (1999) judged the reliability of the available data and graded them accordingly. From the study of the most reliable data they found "a distinct segregation of active and inactive stars into two approximately parallel bands, an active and an inactive one." They called them the A (active) and the I (inactive) sequences. They found that for the old, inactive stars on the I sequence the $\Omega_{cyc}/\omega_{rot}$ is about 6 times larger than for the young, active stars. The two sequences are clearly demonstrated by Brandenburg (1998). They are also seen for the Ca II emission line fluxes.

Lorente & Montesinos (2005) used the selected, high-quality data for their theoretical discussions, trying to understand the increasing cycle periods for increasing rotation periods, and the reason for the different sequences in the relations between P_{cyc} and p_{rot}.

Here we use the same observational data as used by Saar & Brandenburg (1999) and by Lorente & Montesinos (2005), but look at them from a different angle. We base our discussion only on the measured data of P_{cyc} and p_{rot}, without reference to any special numbers from dynamo theory. We only use a qualitative picture of stellar dynamos. We hope that this will help to prevent us from making any unjustified assumptions about the stellar dynamos. It will also make it easier to relate the activity observations to stellar structure and evolution. For this we also discuss the Ca II emission line fluxes and their relation to T_{eff} and p_{rot}.

2. THE OBSERVATIONS

2.1. *The Data*

Table 1 gives the data for the stars studied here. They are the high-quality data, as selected by Saar & Brandenburg (1999),

TABLE 1
BASIC DATA FOR PROGRAM STARS

HR	HD	Spectral Type	m_V	$B-V$	log $T_{\rm eff}$	$p_{\rm rot}$	$P_{\rm cyc}$	$P_{\rm cyc}2$	log $R'_{\rm HK}$	log F(Ca II)	Sequence
4437	100180	F7 V	6.20	0.57	3.7746	14	12.9	3.6	−4.922	5.930	A
4983	114710	F9 V	4.26	0.58	3.7723	12.35	16.6	9.6	−4.745	6.097	A
3625	78366	G0 V	5.93	0.60	3.7676	9.67	12.2	5.9	−4.608	6.216	A
7672	190406	G1 V	5.80	0.61	3.7653	13.94	16.9	2.6	−4.797	6.018	A
88	1835	G3 V	6.39	0.66	3.7536	7.78	9.1	...	−4.433	6.335	A
996	20630	G5 V	4.83	0.68	3.7489	9.24	5.6	...	−4.420	6.329	A
3538	76151	G3 V	6.00	0.67	3.7512	15.	...	2.52	−4.659	6.100	Ab?
	152391	G7 V	6.64	0.76	3.7302	11.43	10.9	...	−4.448	6.226	Ab
3750	81809	K0 V	5.38	0.80	3.7208	40.2	8.2	...	−4.921	5.716	I
4550	103095	G8 V	6.45	0.75	3.7325	31	7.3	...	−4.896	5.788	I
	115404	K1 V	6.52	0.94	3.6880	18.47	12.4	...	−4.480	6.026	Ab, I
6171	149661	K2 V	5.75	0.84	3.7114	21.07	16.2	4.0	−4.583	6.017	Ab, I
	156026	K5 V	6.34	1.16	3.637	21	21.0	...	−4.662	5.638	Ab, I
6752	165341	K1 V	4.03	0.86	3.7068	19.9	15.5	5.1	−4.548	6.033	Ab, I
222	4628	K2 V	5.75	0.88	3.7021	38.5	8.6	...	−4.852	5.710	I
493	10476	K1 V	5.24	0.84	3.7114	38.2	9.6	...	−4.912	5.688	I
	160346	K3 V	6.52	0.96	3.6834	36.4	7.0	...	−4.795	5.692	I
8085	201091	K5 V	5.21	1.17	3.6342	35.37	7.3	...	−4.964	5.327	I
8086	201092	K7 V	6.03	1.37	3.5874	37.84	10.5	...	−4.891	5.212	I
166	3651	K0 V	5.87	0.85	3.7091	44.	14.6	...	−4.991	5.599	I
753	16160	K3 V	5.82	0.98	3.6787	48.0	13.2	...	−4.958	5.510	I
1325	26965	K1 V	4.43	0.82	3.7161	43	10.1	...	−4.872	5.746	I
1614	32147	K5 V	6.22	1.06	3.6560	48	11.1	...	−4.948	5.446	I
6806	166620	K2 V	6.40	0.87	3.7044	42.4	15.8	...	−4.955	5.616	I
8866	219834B	K2 V	?	0.91	3.6951	43	10.0	...	−4.944	5.590	I

and also used by Lorente & Montesinos (2005). The cycle periods, $P_{\rm cyc}$, are given in years, and the rotation periods, $p_{\rm rot}$, in days. For the Ca II emission line fluxes Saar & Brandenburg give the $R'_{\rm HK} = F({\rm Ca\ II})/\sigma T_{\rm eff}^4$. To obtain the F(Ca II) we multiplied the $R'_{\rm HK}$ with $\sigma T_{\rm eff}^4$, using the $T_{\rm eff}\,(B-V)$ relation used by Saar & Brandenburg (1999).

2.2. *Relation between Rotation Periods and Cycle Lengths of Stellar Activity*

In Figure 1 the lengths of the activity cycles, $P_{\rm cyc}$ (in years), are shown as a function of the rotation periods, $p_{\rm rot}$ (in days). As known from the Sun, the cycle lengths may vary from one cycle to the next, see Baliunas & Vaughan (1985). The uncertainty in the cycle lengths may be up to 20%.

Brandenburg et al. already found that two sequences are indicated, the active A sequence and the inactive I sequence. The steep sequence shows more scatter than the flat one and may actually consist of two subsequences, Aa and Ab. The Aa sequence contains four stars with $B-V$ values less than 0.63. They are indicated by squares around their symbols. They cannot be much older than the Sun, or they would not be on the main sequence. The presence of two Hyades group stars on the Aa sequence, indicated by an H, confirms the relative youth of these stars. Several of the A-sequence stars show two activity cycles. Their secondary, shorter cycles are shown by triangles. The position of the Sun is shown by a square with a dot inside. It is situated between the two primary sequences. Clearly along each sequence the $P_{\rm cyc}$ increase with increasing $p_{\rm rot}$.

In Figure 2 the $P_{\rm cyc}$ are shown again as a function of $p_{\rm rot}$, but this time in a double logarithmic plot. The two Hyades group stars are again indicated by an H. The position of the Sun is again shown by the square with a dot inside. The numbers give the $B-V$ values for the stars. Here the symbols for the stars with secondary activity cycles are enclosed in squares. They include

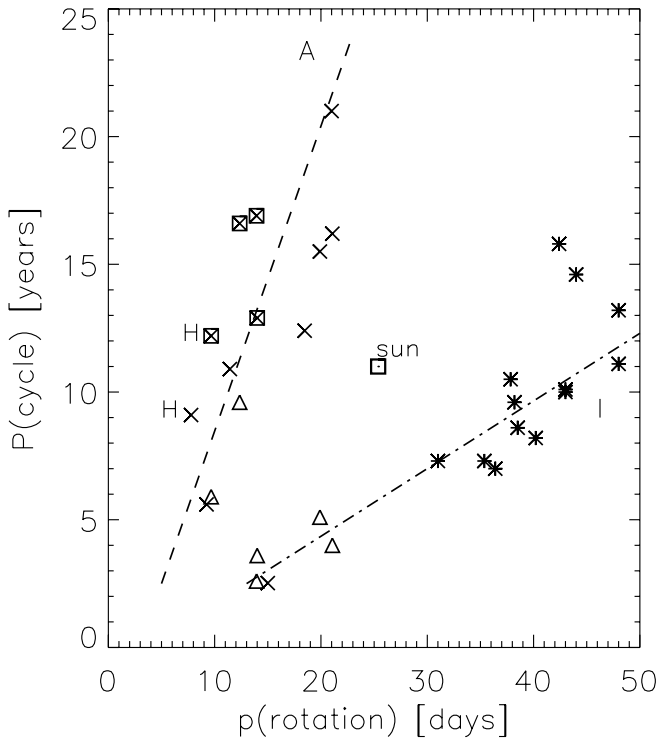

FIG. 1.—Periods of the activity cycles, $P_{\rm cyc}$ in years, are plotted as a function of the rotation periods, $p_{\rm rot}$, in days. The data follow two sequences, the relatively young, active A sequence (*dashed line*) and the generally older, less active I sequences (*dash-dotted line*). The letter H indicates Hyades group stars, crosses indicate stars on the A sequence, and asterisks indicate stars on the I sequence. Squares around the crosses show stars with $B-V<0.62$. Triangles indicate secondary periods for some stars on the A sequence. The solar point is plotted as a square with a dot inside.

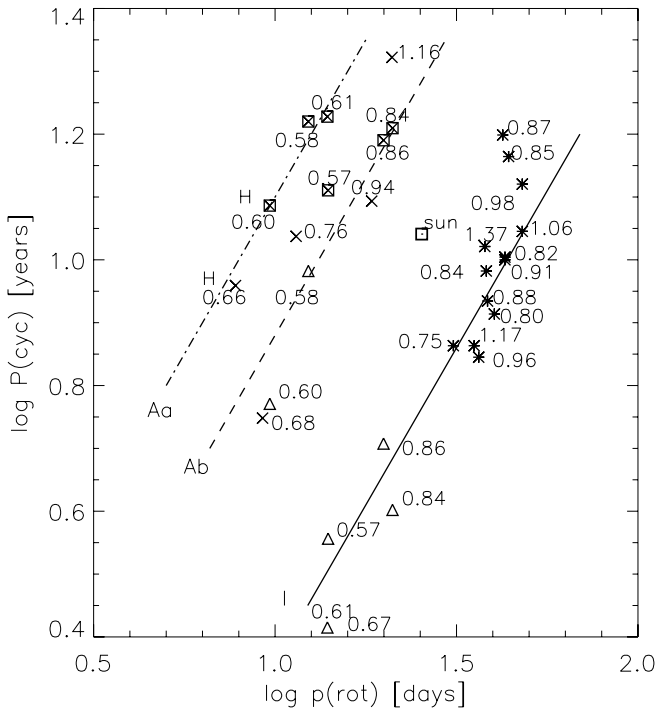

FIG. 2.—Same data as seen in Fig. 1 are shown on logarithmic scales. In this plot the A sequence appears to split up into two subsequences, Aa (*dash-dot line*) and Ab (*dashed line*). The symbols are the same as in Fig. 1, except that here the squares indicate the stars with secondary periods. They include all the stars with $B - V < 0.62$ plus some additional ones. Most of the secondary cycles for some of the A-sequence stars, indicated by triangles, fall along the extended I sequence (*solid line*). The straight lines are eye-fitted linear relations of the form $\log P_{\rm cyc} = C + \log p_{\rm rot}$ with different values of C for the different sequences. The numbers on the symbols give the $B - V$ values for the stars.

all the stars with $B - V < 0.62$. The values for the secondary cycles are shown by triangles. The three suggested sequences now appear as three parallel, straight lines. For each sequence the $P_{\rm cyc}$ are proportional to $p_{\rm rot}$. Except for the Sun, there are very few stars between the main two sequences. Clearly the Sun is not a good standard star for the discussion of stellar activity. (Is its special position between the sequences necessary to permit life on earth to evolve and survive?)

Most of the secondary periods fall on the extrapolation of the I sequence. (For HD 76151, with $B - V = 0.67$, only one cycle was measured. Its value falls, however, on the extended I sequence. It thus seems that the measured cycle length is actually the short secondary cycle. Presumably it also has a longer cycle that has not yet been identified. We treat the measured cycle of this star as the secondary cycle.) For a given star the two cycles are apparently working independently of each other. It thus appears that the secondary activity cycles for the A-sequence stars are generated in a different layer of the star than the first one, which means by a different dynamo, that is feeding on a different velocity gradient than the primary one. This was already suggested by Durney et al. (1981) as a possibility. (They also discussed higher order modes of the dynamo as a possibility, but the ratios of the two periods are very different for different stars.) That most of the secondary periods fall on the I sequence seems to indicate that these secondary activities for the A-sequence stars are generated by the same dynamo that is the primary one for the I-sequence stars. That the I-sequence dynamo can also work in these more rapidly rotating A-sequence stars shows that the difference in rotation periods for the A- and I-sequence stars is not the reason for the different dynamos. The difference must be in the dynamo mechanism, which is correlated with, but not caused by the slower rotation seen for most I-sequence stars. We hypothesize that for the stars on the different sequences different rotation velocity gradients, present in different stellar layers, contribute to different dynamos. Apparently both kinds of dynamos can work simultaneously, but for the A-sequence stars one dynamo is more efficient and for the I-sequence stars the other one is more efficient. We suspect that similar dynamos work for the two A subsequences, but the fact that two secondary cycles of Aa-sequence stars fall on the Ab sequence, shows that there must also be some difference between the workings even of those two dynamos. Generally the stars on the Ab sequence have somewhat longer rotation periods and larger $B - V$ values than those on the Aa sequence. They thus appear to have deeper convection zones. They also may be slightly older than the Aa-sequence stars, because they have somewhat lower rotation velocities.

2.3. *The Ratios of $P_{\rm cyc}$ to $p_{\rm rot}$*

In Figure 2 the gradients for the different sequences are equal, as indicated by the eye fitted straight, parallel lines. For each sequence $\log P_{\rm cyc} = C + \log p_{\rm rot}$, i.e., for each sequence $P_{\rm cyc}$ is proportional to $p_{\rm rot}$. The different sequences are distinguished by different values of C. For a given $P_{\rm cyc}$ the difference $\Delta \log p_{\rm rot}$ between the sequences Aa and I is about 0.65, the difference between sequences Aa and Ab is about 0.2. For a given $p_{\rm rot}$ a difference of $\Delta \log P_{\rm cyc}$ of 0.8 is seen between the two sequences, in agreement with the findings by Saar & Brandenburg, who found a difference of a factor of 6 between the sequences.

The proportionality of $P_{\rm cyc}$ and $p_{\rm rot}$ for each sequence shows that the ratio of $P_{\rm cyc}/p_{\rm rot}$ is constant for each sequence of stars, but different for the different sequences. This ratio is, of course, *the number, n, of rotational revolutions of the star per activity cycle, which is thus nearly the same for all stars on each sequence, but different for the different sequences*.

In Figure 3*a* the number n of rotations per cycle is shown as a function of $\log p_{\rm rot}$ for the stars on the different sequences. For the Aa sequence the number of rotations per cycle is between 400 and 500. It is about 300 for the Ab sequence and about 90 for the I sequence. For the Sun, n comes out to be about 150. There is a clear separation between the $p_{\rm rot}$ of the A an I-sequence stars. The difference between the Aa and Ab sequences is less significant. We suggested above that the dynamos working for the suggested A sequences are similar but that the dynamos for the A and the I sequences are very different. For our picture of the stellar dynamos we expect that for a given gradient of the rotation rates a certain number of rotations is necessary for the magnetic field to reach the required strength that makes the buoyancy of the toroidal field strong enough to bring it to the surface. Depending on the gradients of $p_{\rm rot}$ and perhaps on the depths of the stellar layers in which the dynamos occur, more or fewer rotations are apparently needed for this. We may perhaps expect that the velocity gradients at the bottom of the convection zones are larger for deeper convection zones, and fewer rotations are needed to reach the unstable magnetic field strength. Perhaps this explains why n is smaller for the Ab-sequence stars with deeper convection zones, than for the Aa-sequence stars. It seems that for the I-sequence stars, much deeper mixing has occurred, creating even larger velocity gradients in much deeper layers, such that even fewer rotations are needed to make the toroidal field strong enough to rise.

The Sun is apparently influenced nearly equally by both kinds of dynamos. We may possibly expect to observe some kind of

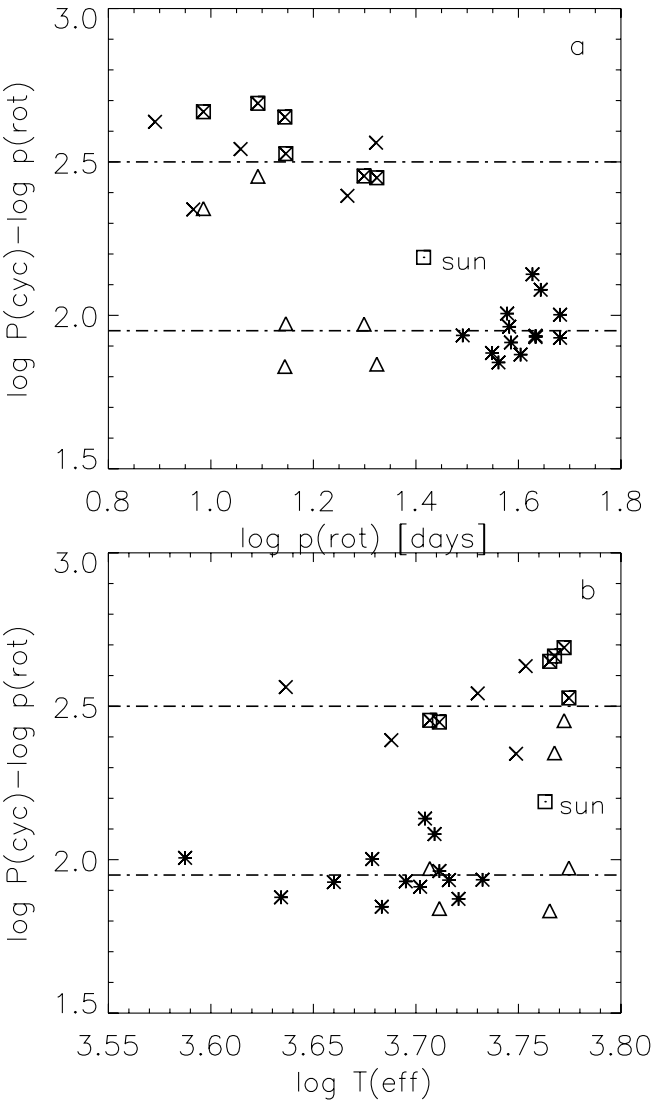

FIG. 3.—(*a*) Logarithms of the ratios $P_{\rm cyc}/p_{\rm rot}$ are shown as a function of $\log p_{\rm rot}$. This ratio gives the number of rotations per cycle. The symbols are the same as in Fig. 2. Within a range of Δ log of about ± 0.15 these numbers are essentially the same for all stars on a given sequence, but are different for the different sequences. The dash-dot lines are only meant to guide the eyes. Except for the secondary cycles, there is a sharp transition from the A sequence to the I sequence for $\log p_{\rm rot} > 1.32$. The Sun falls between the two sequences. (*b*) The logarithms of the ratios $P_{\rm cyc}/p_{\rm rot}$ are shown as a function of $T_{\rm eff}$. Symbols are the same as in Fig. 3*a*. The Sun is always situated between the sequences. For several values of $\log T_{\rm eff} < 3.74$ there are stars on both sequences.

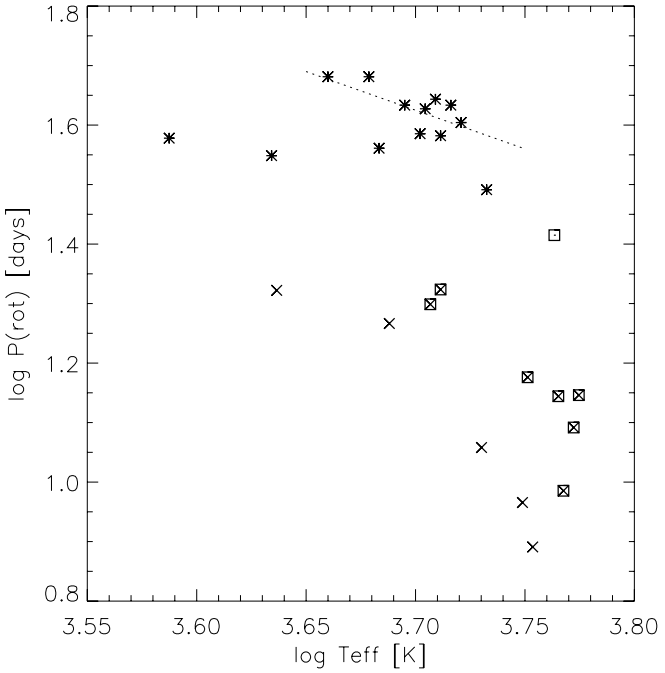

FIG. 4.—Values of $\log p_{\rm rot}$ are shown as a function of $\log T_{\rm eff}$. The symbols are the same as in Fig. 2. The dotted line shows the eye-fitted relation $\log p_{\rm rot} = C - 4/3 \log T_{\rm eff}$. A gap in the distribution for $\log p_{\rm rot} > 1.3$ is obvious. Only the Sun and one G8 star are found in the gap.

beat phenomenon between the two operating cycles with one of about 90 rotations and the other one with 315 rotations per cycle. If both dynamos are in phase the activity will be especially strong. We speculate that perhaps this may lead to the additional, longer cycles of activity, that were found for the Sun by different earlier studies, for instance Gleissberg (1944). (Two long cycles require 630 rotations. During this time seven short cycles with 90 rotations have passed. We may thus expect especially strong cycles after every 630 rotation periods. With a solar rotation period of 25.4 days, as quoted by an unknown referee, we expect strong cycles every 630 times 25.4 days = 43.8 yr, which is about half the length of the Gleissberg cycle of about 80 yr. With neither cycle being well determined it seems quite possible to me that one maximum may have been too poorly defined and may thus have been missed. Somewhat different numbers of n for the two dynamos can also lead to beat cycles with periods of about 80 yr, for instance $n1 = 299$ and $n2 = 92$ leads to a beat period of 83.2 yr, and $n2 = 88$ and $n1 = 286$, to a beat cycle of 79.6 yr. Due to the interaction of the two cycles the lengths of the solar cycles will vary. The longer cycle seems to contribute less to the activity than the shorter one. If the long one is at a minimum, we may mainly see the short one with a length of about 6.4 yr, always adopting the solar rotation period of 25.4 days.

In Figure 3*b* the number of rotations per cycle is shown again, but as a function of $T_{\rm eff}$. For some $\log T_{\rm eff} < 3.73$ both, A- and I-sequence stars may be found for the same $T_{\rm eff}$. The transition to deeply mixed stars does not seem to occur for a well-defined $T_{\rm eff}$, but rather for a well defined $p_{\rm rot}$.

3. THE RELATION BETWEEN $p_{\rm rot}$ AND $T_{\rm eff}$

For the comparison with stellar structure models it is helpful to know the relation between $p_{\rm rot}$ and $T_{\rm eff}$ for the stars studied here. In Figure 4 this relation is shown. The gap in rotation velocities between the I and the A sequence is striking. For $T_{\rm eff} <$ 5400 K there are no stars with $\log p_{\rm rot}$ between 1.35 and 1.55, except for the Sun and one G8 star. Both seem to be in transition from one sequence to the other. For each $T_{\rm eff}$ there is between sequence A and sequence I an abrupt increase in $p_{\rm rot}$ by a factor of about 1.6. We suspect that the I-sequence stars experienced deep mixing that transferred angular momentum from the surface layers to deep layers, thereby reducing the surface rotation rate. (A small gap seen in the Hyades main sequence around $B - V = 0.7$; see de Bruijne 2000), may possibly be related to this additional mixing.

If the mixing is deep enough surface abundance changes may be observed. For giants with $T_{\rm eff}$ around 6300 K a reduced Li surface abundance is correlated with decreased surface rotation (Böhm-Vitense 2004). For giants with $T_{\rm eff}$ around 5000 K, increased N/C abundance ratios are also correlated with decreased surface rotation. For main-sequence field stars, as studied here,

TABLE 2
Basic Data for Differential Rotation Stars

HD	Spectral Type	$B-V$	$\log T_{\rm eff}$	$p_{\rm rot}$	$\log p_{\rm rot}$	$p_{\rm rot}$ Minimum	$p_{\rm rot}$ Maximum
114710	F9.5 V	0.58	3.772	12.35	1.09	11.43	13.54
78306	G0 V	0.60	3.768	9.67	0.99	9.12	10.19
190406	G1 V	0.61	3.765	13.94	1.23	12.67	15.57
1835	G3 V	0.66	3.754	7.78	0.89	7.23	8.30
2063	G5 V	0.68	3.749	9.24	0.97	9.01	9.48
152391	G7 V	0.76	3.730	11.43	1.06	10.2	12.97
81809	K0 V	0.80	3.721	40.2	1.60	37.0	43.0
10476	K1 V	0.84	3.771	35.2	1.55	34.0	37.3
149661	K2 V	0.84	3.711	21.07	1.32	20.6	22.9
166620	K2 V	0.87	3.704	42.4	1.63	33.4	50.8
4628	K2 V	0.88	3.702	38.5	1.59	37.2	41.4
115404	K1 V	0.94	3.688	18.47	1.266	17.24	19.90
160346	K3 V	0.96	3.683	36.4	1.56	35.4	37.8
16160	K3 V	0.98	3.679	48.0	1.68	42.2	51.5
201091	K5 V	1.17	3.634	35.37	1.55	26.82	45.25
201092	K7 V	1.37	3.587	37.84	1.58	31.78	46.57

changes in the N/C surface abundance ratios are not observed. The mixing apparently does not go deep enough. Any additional mixing will, however, increase the velocity gradient at the bottom of the deep, mixed layer.

Figure 4 shows that for most of the I-sequence stars at most a small increase of $p_{\rm rot}$ with decreasing $T_{\rm eff}$ may be indicated. The eye-fitted dotted line suggests a dependence $p_{\rm rot} \propto T_{\rm eff}^{-1.33}$ (see also § 4.2). For the coolest stars no such increase in $p_{\rm rot}$ is seen.

The stars on the A sequence show a strong, systematic increase of $p_{\rm rot}$ with decreasing $T_{\rm eff}$. Also the stars with secondary cycles have, for a given $T_{\rm eff}$, larger $p_{\rm rot}$ than the other early G stars. This shows that even for these A-sequence stars probably a limited amount of deeper mixing occurred, just enough to enable the second dynamo to work in deep layers creating secondary activity cycles that match the I sequence.

3.1. *Differential Rotations*

The amount of differential rotation of G and K main-sequence stars was studied by Donahue (1993) and Donahue et al. (1996). Lorente & Montesinos (2005) list minimum and maximum $p_{\rm rot}$ for most of the stars in their Table 1. These stars and their rotational data are listed in Table 2. For each star we have divided the difference of the minimum and maximum $p_{\rm rot}$ values by their average, to determine the fraction of its differential rotation. In Figure 5 the fractional differences are shown as a function of $p_{\rm rot}$. The relative differential rotation rates appear to have a minimum for $\log p_{\rm rot}$ around 1.4, where the gap in $p_{\rm rot}$ is found. The differential rotation increases steeply for rotation periods $\log p_{\rm rot} > 1.5$. The largest differential rotations were observed for two late-K stars with $B-V = 1.17$ and 1.37. We suspect that these large differential rotations may be due to a new surface convection zone, due to strong molecular absorption and some dissociation of abundant molecules.

4. CHROMOSPHERIC Ca II EMISSION-LINE FLUXES

4.1. *The Relation between the F*(Ca II) *and* $p_{\rm rot}$

In Figure 6 the $\log F$(Ca II) are shown as a function of $\log p_{\rm rot}$. The numbers given are the $B-V$ values. As in Figure 2, the three sequences are seen, but, of course, the F(Ca II) decrease for increasing rotation periods. The Aa and I sequences are again parallel, but the Ab sequence seems to be somewhat flatter. The coolest Ab stars seem to be in transition from the Ab to the I sequence, which happens for $\log p_{\rm rot}$ of about 1.3. (This means it happens when the rotation velocities decrease below the convective velocities, which are near 2 km s^{-1}. We do not know whether this has any significance, except that it reduces the differential rotation as seen in Fig. 5.) The transition from the A to the I sequence is again rather abrupt, leaving a gap between the Ca II emission line fluxes for the two sequences. This separates the "active" from the "inactive" stars. (Only the Sun is found in the gap.) For $B-V < 1.1$ there is no overlap of the $p_{\rm rot}$ for the two sequences, but, surprisingly, the Ca II emissions for the lowest temperature I-sequence stars fit on the extrapolated Aa sequence. For a given $p_{\rm rot}$ the F(Ca II) for the I-sequence stars are about a factor of 3 larger than expected for the extrapolated Aa sequence,

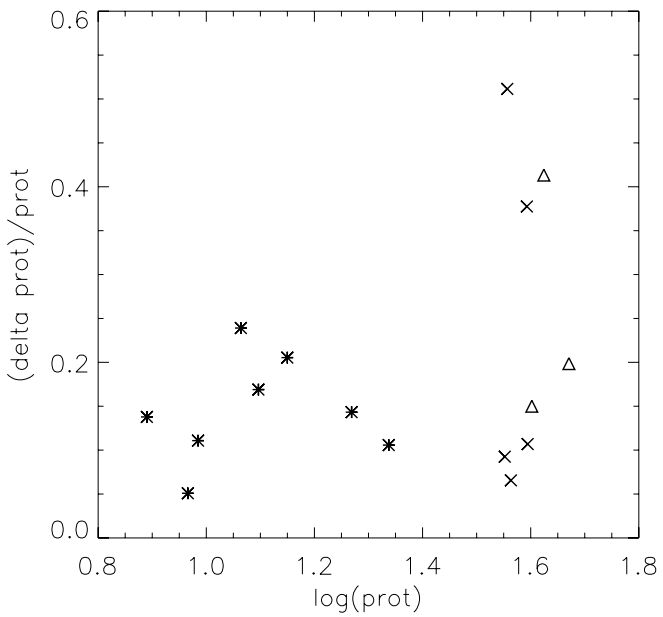

Fig. 5.—Differential rotations, as measured by Donahue (1996), are plotted as a function of $\log p_{\rm rot}$. Asterisks indicate the highest degrees of reliability, and triangles indicate the lowest degree (see Lorente & Montesinos 2005).

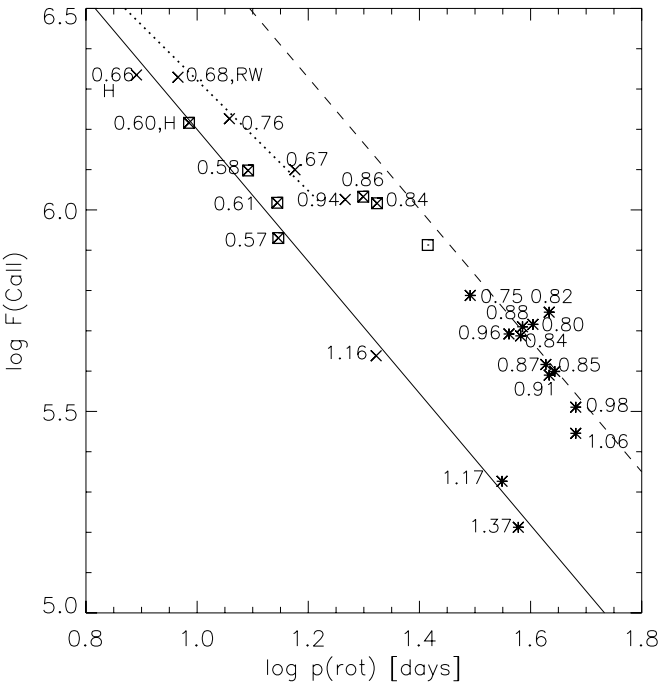

FIG. 6.—On a double logarithmic scale the Ca II emission line fluxes, F(Ca II), are shown as a function of $p_{\rm rot}$. The symbols are the same as in Fig. 2. The numbers given are the $B - V$ values. The three sequences, seen in Fig. 2, are also seen here. The fluxes decrease for increasing $p_{\rm rot}$ (or decreasing $V_{\rm rot}$). The straight lines show an eye-fitted power-law dependence. The Aa and I sequences are parallel.

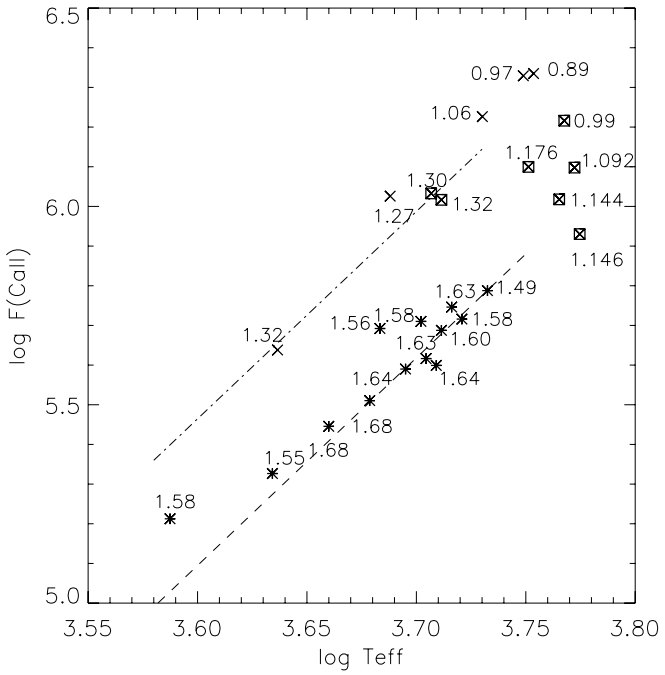

FIG. 7.—In a double logarithmic scale the Ca II emission line fluxes are shown as a function of $T_{\rm eff}$. Symbols are the same as in Fig. 2. The numbers give the $\log p_{\rm rot}$. For the A-sequence stars the F(Ca II) have a maximum for $\log T_{\rm eff} = 3.75$, for which $\log p_{\rm rot}$ is smallest. The F(Ca II) decrease for higher and lower $T_{\rm eff}$, for which the $p_{\rm rot}$ increase. For $\log p_{\rm rot}$ around 1.3, the transition period, the cool star points on the extended Aa star sequence follow the dash-dot line parallel to the I sequence, but shifted to lower temperatures. For the I-sequence stars the F(Ca II) increase $\propto T_{\rm eff}^{5.3}$ (*dashed line*).

on which the coolest I-sequence stars (as determined by the $P_{\rm cyc}/p_{\rm rot}$) are found.

4.2. *The Dependence of* F(Ca II) *on* $T_{\rm eff}$ *and* $p_{\rm rot}$

In Figure 7 the log F(Ca II) are shown as a function of $T_{\rm eff}$. The numbers given are the $\log p_{\rm rot}$. For the stars discussed here, the largest F(Ca II) are observed for A-sequence stars with $\log T_{\rm eff} = 3.75$. For our sample of stars these are the stars with the shortest rotation periods. For higher and lower $T_{\rm eff}$ the rotation periods increase and the F(Ca II) decrease. For the A-sequence stars the F(Ca II) are thus mainly determined by the rotation periods. For the A-sequence stars Figure 4 shows a strong correlation between $T_{\rm eff}$ and $p_{\rm rot}$. For these stars it is therefore difficult to separate the influence of $p_{\rm rot}$ and $T_{\rm eff}$ on the Ca II emission; however, for a given rotation period the F(Ca II) do not seem to increase for higher temperatures. For the A stars there are too few data to accurately determine the dependences of F(Ca II) on $T_{\rm eff}$ for constant $p_{\rm rot}$, and on $p_{\rm rot}$ for constant $T_{\rm eff}$. There are, however, a number of A-sequence stars within a log $T_{\rm eff}$ interval of 0.02. From these we estimate that F(Ca II) is perhaps proportional to $p_{\rm rot}^{-x}$, where x is about $4/3 \pm 1/3$.

As seen in Figure 4, very little dependence of $p_{\rm rot}$ on $T_{\rm eff}$ is seen for the I-sequence stars, although, as shown by the dotted line, for $\log T_{\rm eff} > 3.65$ an increase of $p_{\rm rot}$ for decreasing $T_{\rm eff}$ proportional to $T_{\rm eff}^{-4/3}$ is likely. The decreasing F(Ca II) for decreasing $T_{\rm eff}$ must therefore mainly be attributed to the changes in $T_{\rm eff}$. Figure 7 shows that to within ± 0.05 in the log the F(Ca II) for these stars are roughly proportional to $T_{\rm eff}^{5.3}$. The dashed and the dash-dot lines show these relations for the I sequence and a few cool stars near or on the extended A sequence. Assuming that for the I-sequence stars F(Ca II) is inversely proportional to the rotation period we derive that F(Ca II) $\propto T_{\rm eff}^{4}/p_{\rm rot}$ or $\propto T_{\rm eff}^{5.3}$, consistent with the observations.

5. SUMMARY AND DISCUSSION

5.1. *The Vaughan-Preston Gap in the* Ca II *Emission-Line Fluxes*

When plotting the chromospheric Ca II emission line index S as a function of $B - V$, Vaughan & Preston (1980) saw two branches with a gap between them, now called the Vaughan-Preston gap. Vaughan & Preston called the two branches the active, young one and the less active, old one. They discussed whether the gap might be due to a pause in star formation in the solar neighborhood but rejected it as rather unlikely.

In 1981 Durney et al. discussed the possibility of two different dynamos, each working mainly for one branch. These authors preferred, however, another possibility than suggested here, namely, a change in the morphology of the magnetic field. They suggested that for earlier spectral types the field would consist of many small-scale fields. For later spectral types these would change to a global field. They hypothesized that at the transition $T_{\rm eff}$, strong stellar winds would occur, which would brake the stellar rotation. However, no signs of such strong winds have been observed, nor has especially strong X-ray emission been observed, which would be expected for high-temperature coronae causing such strong winds.

5.2. *The Reason for the Two Sequences of Stellar Activity*

Thanks to the observations of Wilson, Baliunas, Vaughan, and others we have now a reasonably large number of observations of reliable rotation periods and activity cycles.

As seen in Figures 1 and 2, the observed relation between rotation periods and lengths of activity cycles for main-sequence G and K stars also shows mainly two sequences, which Saar & Brandenburg called the active, A, and the inactive, I, sequences.

Vaughan and Preston called the two groups with different F(Ca II) the young and the old one. Here we see that for the two sequences the ratios of $P_{\rm cyc}/p_{\rm rot}$ are different, showing that different dynamos are working for the two sequences. This was also suggested by Durney et al. (1981) as one of the possibilities to understand the Vaughan and Preston gap.

Figure 2 shows that the transition from one sequence to the other is correlated with a decrease in rotation for $B-V$ larger than about 0.7, or, more accurately, for $\log p_{\rm rot} > 1.3$. Durney et al. (1981) also suggested as another possibility that the character of convection may perhaps change, if the rotational velocities become smaller than a certain limiting value. The fact that the transition occurs at a $p_{\rm rot}$ for which the rotation velocity becomes comparable to the convective velocity, makes this suggestion attractive. Theory has shown that for rotating stars convective cells are expected to be long cylinders rather than "bubbles." Cylinders might then be expected for more rapid rotation. Figure 3 showed that for the more rapidly rotating stars a larger number of rotations per cycle is required for the dynamo to work. But why should this be necessary for cylindric convection cells? It is also not obvious how the change from cylinders to bubbles can lead to a sudden reduction in surface rotation, as is observed. According to Figures 2 and 3 the Sun seems to be in transition from one sequence to the other. It should then probably show some cylindric convection and some "bubbles." Observations do not show any indication of convective cylinders in the Sun.

A decrease of surface rotation may also happen due to an extension of mass motions into deeper layers. These transport angular momentum from the surface to the deeper layers, as discussed by Endal & Sofia (1978), and by Böhm-Vitense (2004). For giants this is observed for $T_{\rm eff}$ around 6300 K, where the Li abundances decrease steeply, combined with a decrease in rotation velocities, and for temperatures around 5000 K, where the surface N/C abundance ratio increases with decreasing rotation. If increased mixing is the explanation for the transition of the main-sequence K stars from the A sequence to the I sequence, it must for these stars occur for $T_{\rm eff}$ around 5300 K. It appears that in this temperature range the convection zone depth grows rapidly. Perhaps this may explain the rapid increase in $p_{\rm rot}$. As seen in Figure 2, the transition occurs, however, not over a very narrow temperature range but rather at a given value of surface rotation, as seen in Figure 4. A search for other signs of deep mixing, like changes in surface abundances, may help to solve this problem. Such observations may thus help to determine accurately the temperature stratification in the deep layers of the K star convection zones and the dependence on rotation.

5.3. *The Stellar Dynamos*

The recent determinations of the rotation periods and cycle periods has given us new insights into the characters of the stellar dynamos. The two sequences, formerly found for the Ca II emission-line fluxes, when plotted as a function of $B-V$, are also seen for the relation between rotation periods and activity cycles. Figure 3 shows that for the two sequences the ratios of $P_{\rm cyc}/p_{\rm rot}$ are different, indicating that different dynamos are at work.

Stellar dynamos work in the presence of either latitudinal or radial gradients of the rotation periods. In these cases rotation winds up poloidal magnetic field lines, which are frozen into the matter, and creates a toroidal field of increasing field strength until this is strong enough to make the field rise to the surface due to its buoyancy. (Due to the Coriolis force a new, a weak poloidal field is recreated from the toroidal field on the way up.) The number of rotations necessary to reach this instability supposedly determines the length of the activity cycle. Kinematic dynamo theory tells us that for stars with similar structure the number of rotations per cycle should be the same, as is observed here for the stars of each sequence (see for instance the discussion by Noyes et al. 1984). The observed numbers are, however, different for the two sequences, telling us that the relevant stellar structures and/or the dynamos are different for the two sequences.

The observations give only a few hints about the specific properties of the different dynamos. The A-sequence dynamo requires many rotations per cycle, which probably means it works with relatively thin convection zones (small convective turnaround times) and small rotation gradients, as are present for the differential rotation, which is due to the interaction of convection and rotation. (Possibly the vertical gradient of $p_{\rm rot}$ near the surface, as derived for the Sun by Benevolenskaya et al. [1999] from helioseismology, also contributes.) Figure 5 suggests that the differential rotation has a minimum for $\log p_{\rm rot}$ around 1.4. At $p_{\rm rot} = 1.3$ the A sequence stops, the rotation periods abruptly increase, and the more slowly rotating K stars with deeper mixed zones appear on the I sequence. That these changes occur near the minimum for the differential rotation seems to confirm that for the A-sequence stars differential rotation near the surface mainly feeds their dynamos.

The large increase in differential rotations, observed for the late-K stars, probably indicates increased convective velocities near the surface and increased importance of a surface dynamo. This can possibly be attributed to a new surface convection zone, due to molecular absorption and dissociation.

For the I-sequence stars the surface rotational velocities have apparently abruptly been reduced by nearly a factor of 2. If this was achieved by increased deep mixing, the largest vertical differences in $p_{\rm rot}$ are expected at the bottom of the mixed layer. These interface gradients in $p_{\rm rot}$ are probably much larger than the latitudinal differences of $p_{\rm rot}$ near the surfaces. Therefore, fewer rotations suffice to create a toroidal magnetic field strong enough to make it rise to the surface. We suggest that these interface dynamos in the stars with deep, mixed layers are the important ones for the I-sequence stars. The toroidal magnetic fields then have to rise to the surfaces through thick layers of stellar material. On the way up they are weakened by dissipative effects. Nevertheless, for a given $p_{\rm rot}$ the interface dynamo seems to lead to larger Ca II emission line fluxes than expected for a surface dynamo with similar rotation rates.

The secondary activity cycles, mainly observed for stars with $\log p_{\rm rot} < 1.3$, can probably also be attributed to interface dynamos working at the bottoms of shallow convection zones in the early G stars, with possibly smaller gradients of $p_{\rm rot}$ than in the K stars, but with smaller rotation periods and probably smaller instability limits for the toroidal field than for the deep interface dynamo.

5.4. *The Dependence of F*(Ca II) *on $T_{\rm eff}$ and $p_{\rm rot}$*

The condition of radiative equilibrium for the stellar photospheres tells us that the chromospheres are not heated by the photospheric radiation, but must be heated by some so-called mechanical energy. The kinetic, mechanical energy flux of the photospheric convection is believed to be the main source of this energy. Magnetic energy is another possible source of nonradiative energy. The convective kinetic energy flux per unit surface area and per second is proportional to v^3. Theory tells us (Böhm-Vitense 1958) that the total convective energy flux per unit surface area and per second, $F_{\rm conv}$, is also proportional to v^3. If in the convection zone, $F_{\rm conv}$ nearly equals the total energy transport, $\sigma T_{\rm eff}^4$, we

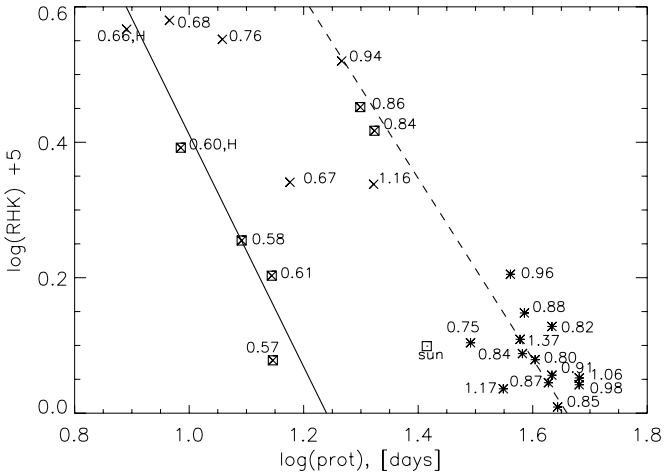

FIG. 8.—R'_{HK} are shown as a function of the rotation periods. The numbers give the $B - V$ values. The eye-fitted solid line gives the relation $R'_{HK} \propto p_{rot}^{-4/3}$ for the I sequence. The dashed line shows the relation $R'_{HK} \propto p_{rot}^{-1.72}$ for the A sequence.

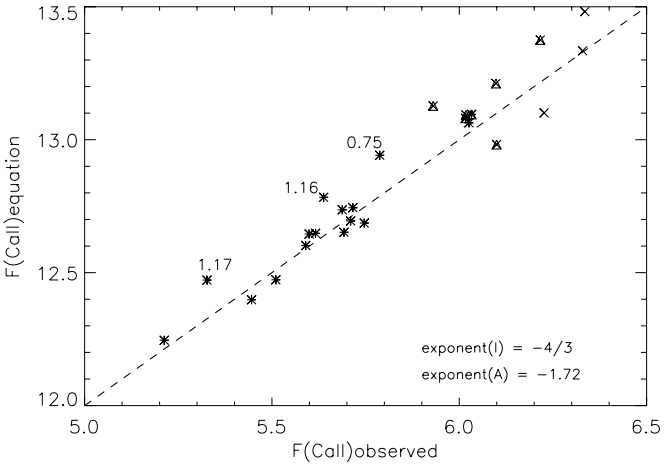

FIG. 9.—Values of F(Ca II), calculated according to eq. (1), are shown as a function of the observed F(Ca II)obs. With the proportionality factor of 10^{-7} the points for both sequences lie close to the dashed line.

find that the kinetic energy flux, available to heat the chromosphere, is proportional to T_{eff}^4. This explains why the F(Ca II) are proportional to T_{eff}^4, if the heating is mainly due to the convective mechanical energy. The magnetic energy is supposedly a function of p_{rot}. We thus assume that the heating and thereby the F(Ca II) is proportional to $T_{eff}^4 p_{rot}^x$, where x needs to be determined. *If* this is so, then we can determine p_{rot}^x by dividing the F(Ca II) by σT_{eff}^4, which means by using the R'_{HK}. Figure 8 shows the R'_{HK} as a function of p_{rot}. The A and the I sequences are clearly distinguished. The eye-fitted straight line through the I sequence gives the relation $R'_{HK} \propto p_{rot}^{-4/3}$. For the A sequence the parallel line appears to be too flat. The solid line shown corresponds to $x = -1.72$.

We note that the stars with $B - V = 0.94, 0.86, 0.84$, and 1.16, which according to Figure 2 belong to the Ab sequence, appear here on the I sequence for the F(Ca II). This apparently means that the cycle length is mainly determined by the surface dynamo, but that the Ca II emission is mainly determined by the interface dynamo. We treat these stars in this context as I-sequence stars.

In Figure 9 the $\log F$(Ca II), calculated from the equation

$$\log F(\text{Ca II}) = \log T_{eff}^4 - x \log p_{rot}, \qquad (1)$$

are plotted as a function of the observed F(Ca II). $x = 4/3$ was used for the I sequence, and $x = 1.72$ was used for the A sequence. [This assumes that for the A sequence the F(Ca II) are also proportional to T_{eff}^4. This still has to be verified.] With a proportionality constant of 10^{-7} the $\log F$(Ca II), calculated with equation (1), agree with the observed F(Ca II), confirming that for the A-sequence stars the F(Ca II) have a stronger dependence on $\log p_{rot}$ than the I-sequence stars. The close agreement for all stars, seen in Figure 9 is surprising, because the stars have almost certainly different ages. Either there is essentially no age dependence or perhaps the age dependence is absorbed in the dependence on p_{rot}, which appears to decrease with increasing age. In which way the magnetic field influences the Ca II emission does not seem to be understood yet, but solar observations show that the Ca II emission is stronger in areas with stronger magnetic fields.

Interesting discussions with Suzanne Hawley and George Wallerstein helped to improve the manuscript.

REFERENCES

Babcock, H. 1958, ApJS, 3, 141
———. 1961, ApJ, 133, 572
Baliunas, S. L., & Vaughan, A. H. 1985, ARA&A, 23, 379
Baliunas, S. L., et al. 1995, ApJ, 438, 269
Benevolenskaya,E. E., Hoeksema, J. T., Kosovichev, A. G., & Scherrer, P. H. 1999, ApJ, 517, L163
Böhm-Vitense, E. 1958, Z. Astrophys., 46, 108
———. 2004, AJ, 128, 2435
Brandenburg, A. 1998, in ASP Conf. Ser. 154, The 10th Cambridge Workshop on Cool Stars, ed. R. A. Donahue, & J. A. Bookbinder (San Francisco: ASP), 173
———. 2005, ApJ, 625, 539
Brandenburg, A., Saar, S. H., & Turpin, C. J. 1998, ApJ, 498, L51
de Bruijne, J. H. J., 2000, Ph.D. thesis, Univ. heiden
Donahue, R. A. 1993, Ph.D. thesis, New Mexico State Univ.
———. 1996, in IAU Symp. 176, Stellar Surface Structure, ed. K. G. Strassmeier & J. L. Linsky. (Dordrecht: Kluwer), 261
Donahue, R. A., Saar, S. H., & Baliunas, S. L. 1996, ApJ, 466, 384
Durney, B. R., Mihalas, D.& Robinson, R. D., 1981, PASP, 93, 537
Endal, A. S. & Sofia, S. 1978, ApJ, 220, 279
Gleissberg, W. 1944, Publ. Istanbul Univ. Obs. No 27
Lorente, R. & Montesinos, B., 2005, ApJ, 632, 1104
Noyes, R. W., Weiss, N. O., & Vaughan, A. H. 1984, ApJ, 287, 769
Saar, S. H. & Brandenburg, A. 1999, ApJ, 524, 295
Vaughan, A. H., & Preston, G. 1980, PASP, 92, 385
Weber, E. J., & Davis, L., Jr. 1967, ApJ, 148, 217
Wilson, O. 1978, ApJ, 226, 379